

Shift Speed Improvement of a Metal Belt CVT

Heera Lee

Graduate School, Department Dept. of Mechanical Design Engineering, Sungkyunkwan University,
Kyunggi-do 440-746, Korea

Hyunsoo Kim*

Department of Mechanical Design Engineering, Sungkyunkwan University, Kyunggi-do 440-746, Korea

This paper presents a CVT line pressure control strategy for the increased shift speed. Firstly, an algorithm to increase the CVT shift speed is suggested based on a modified CVT shift dynamics and shift speed maps are constructed. In addition, simplified dynamic models of the line pressure and the ratio control valve are derived by considering the CVT shift dynamics, and low level control algorithms for the ratio and the line pressure control are proposed. Using the shift speed maps and the simplified dynamic models of the CVT system, shift performance is investigated. It is found from the experimental and simulation results that improved shift speed can be achieved by increasing the line pressure.

Key Words : CVT (Continuously Variable Transmission), Line Pressure, Shift Speed

1. Introduction

In a metal belt continuously variable transmission (CVT), line pressure is required to supply a clamping force between the belt and pulley. Insufficient line pressure causes a gross slippage of the belt, which results in a loss of power transmission capability. On the other hand, excessive line pressure causes a hydraulic loss as well as a short life of the belt. Since the line pressure can be increased up to 50 bars in the metal belt CVT, the hydraulic loss due to the high line pressure contributes to a major powertrain loss. Consequently, the line pressure control is considered to be an integral part of the CVT design, and many researches and developments on the CVTs have been focused on mostly how to provide an optimal pressure (Fujii, T, 1993; Lee, H and Kim, H, 2000) and on the related control strategies

(Funatsu, K, 1996; Sato, 1996; Kim, T and Kim, H, 2000) to minimize the hydraulic loss due to the high line pressure.

It is well known that the CVT shift speed depends on magnitude of the primary pressure as well as the pressure difference in the actuator (Ide, T, 1995). Since most CVTs developed so far adopt speed ratio control systems which supply the primary actuator pressure by reducing the line pressure, the maximum primary pressure that affects the shift speed is limited to the line pressure.

The CVT shift speed is directly related to the vehicle performance such as kickdown maneuver, shift quality, etc. In addition, if we are able to increase the shift speed, the engine operation can be maintained on the optimal operation region which results in the improvement of the fuel economy.

In this paper, a CVT line pressure control strategy is suggested in order to improve the shift speed. A CVT shift speed map is constructed based on the CVT shift dynamics, and simplified dynamic models of the line pressure control valve and ratio control valve are derived including the CVT shift dynamics. Using the dynamic models

* Corresponding Author,

E-mail : hskim@me.skku.ac.kr

TEL : +82-31-290-7438; FAX : +82-31-290-5849

School of Mechanical Engineering, Sungkyunkwan University, Kyunggi-do, 440-746, Korea. (Manuscript Received February 21, 2001; Revised September 17, 2001)

and the shift speed map, model based low level line pressure control algorithm and ratio control algorithm are suggested and performance of the CVT shift speed are investigated by simulation and experiment.

2. Line Pressure and CVT Shift Speed

The CVT shift dynamics is represented as (Ide, T, 1995).

$$\frac{di}{dt} = \beta(i) \omega_p (P_p - P^*_p) \tag{1}$$

where di/dt is the shift speed, $\beta(i)$ is the coefficient which depends on the speed ratio i , ω_p is the primary speed, P_p is the applied primary pressure, P^*_p is the primary pressure at a steady state. Rearranging Eq. (1) gives,

$$\begin{aligned} \frac{di}{dt} &= \beta(i) \omega_p (P_p - P^*_p) \\ &= \beta(i) \omega_p P_p \left(1 - \frac{P^*_p}{P_p}\right) \\ &= \beta(i) \omega_p \frac{F_p A_s}{F_s A_p} P_s \left(1 - \frac{P^*_p}{P_p}\right) \tag{2} \\ &= \alpha(i) \omega_p P_s \left(1 - \frac{P^*_p}{P_p}\right) \end{aligned}$$

where $\alpha(i) = \beta(i) F_p A_s / F_s A_p$. F and A denote the thrust and the actuator area, and subscripts p and s denote the primary and secondary, respectively. The thrust ratio F_p/F_s is known as a function of speed ratio i .

It is noted from Eq. (2) that the shift speed can be increased by increasing the line pressure P_s . Figure 1 shows a shift speed map for various line pressures when the upshift is carried out from a drive-off gear ratio, $i=2.48$. The shift speed map is constructed from the CVT shift dynamics, Eq. (2) at $\omega_p=2000$ rpm. In calculating the shift speed, a safety factor 1.3 for the line pressure is used to guarantee the torque capacity of CVT. When the line pressure P_s is 25bar, the primary pressure P^*_p at a steady state is obtained as $P^*_p=10$ bar (point A) from the line of $di/dt=0$. If we carry out the upshift from A by increasing the primary pressure to the line pressure $P_s=25$ bar, the maximum upshift speed obtainable is

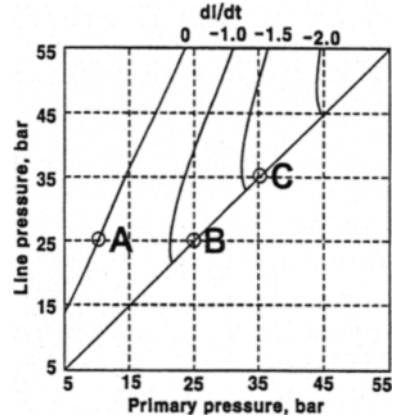


Fig. 1 Shift speed map for upshift case from $i=2.48$

determined as $di/dt=-1.1$ (point B). From the shift speed map, it is obvious to achieve an increased shift speed by increasing the line pressure. For example, if we increase the line pressure up to 35bar (point C), the shift speed obtainable becomes $di/dt=-1.6$.

The shift speed map for the downshift case is shown on Fig. 2. The shift speed map is constructed when the downshift is carried out from the highest gear ratio, $i=0.49$. The primary speed is maintained at $\omega_p=2000$ rpm. At the highest gear ratio, the primary pressure P^*_p at a steady state maintains 25 bars which is equal to the line pressure (point P). The downshift can be performed by reducing the primary pressure or by increasing the line pressure. For instance, if we decrease P_p to 15 bars (point Q), the shift speed $di/dt=2.0$ can be achieved. When a faster shift speed, for example, $di/dt=6.0$ is desired, it is possible to achieve it by the following two ways; one is to reduce the primary pressure down to $P_p=7$ bars. However, an excessive reduction in the primary pressure may cause a belt slippage. The other way is to increase the line pressure up to 52 bars (point R).

The shift speed map can be constructed similarly with various speed ratios for the upshift and the downshift case, and an improved shift speed can be achieved by increasing the line pressure based on the shift speed map.

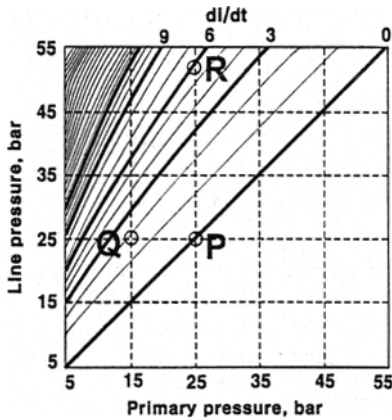


Fig. 2 Shift speed map for downshift case from $i = 0.49$

3. CVT System Modeling

In Fig. 3, schematic diagram of an electronically controlled CVT used in this study is shown. The line pressure is regulated by the line pressure control valve (LCV), which is operated by a variable force solenoid (VFS) type line pressure control solenoid valve (LCSV). The LCSV generates a control pressure P_c which is applied to the land #1 of the LCV spool. If the input duty decreases, P_c increases and the spool moves to the right side to close the exhaust port, which results in the increased line pressure. If the input duty increases, P_c decreases and the decreased line pressure is obtained. So, the line pressure control is achieved by the LCSV duty control. The ratio control valve (RCV) is also operated by the VFS type ratio control solenoid valve (RCSV). If the input duty increases, the control pressure applied to the land #2 of the RCV spool decreases, so the spool moves to the left side. This causes the exhaust port to open, thus the primary pressure decreases and the belt pitch radius decreases, which results in the downshift of the CVT ratio. The upshift can be obtained by decreasing the duty ratio of the RCSV.

In this study, considering the ineffective duty region of the VFS valves and the oil pump flow characteristics, the LCV is modeled as the following second order system.

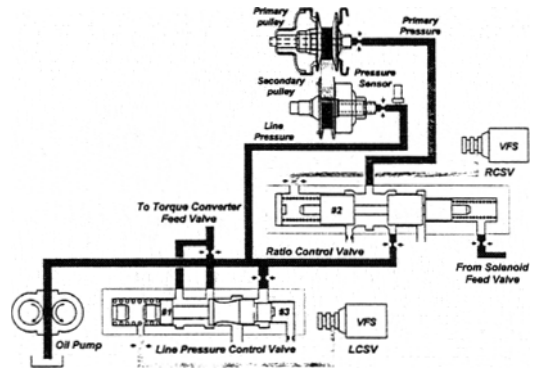


Fig. 3 Schematic diagram of an electronic controlled CVT

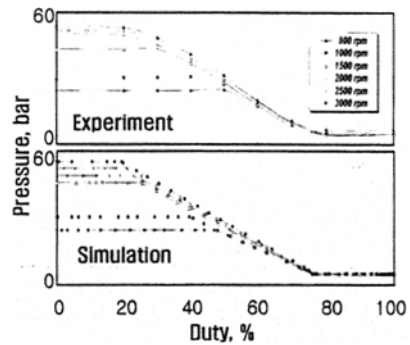


Fig. 4 Steady state characteristics of LCV

$$P_s = \frac{K_1(\omega_{pump}) \omega_n^2}{s^2 + 2\zeta\omega_n s + \omega_n^2} duty + K_2(\omega_{pump}) \quad (3)$$

where K_1 and K_2 are the coefficients depending on the oil pump speed, ζ is the damping coefficient, ω_n is the natural frequency. K_1 , K_2 , ζ and ω_n are determined from the experiments. Figure 4 shows a comparison of the simulation results for the LCV steady state characteristics with the experimental results. As shown in Fig. 4, the effective duty range where the line pressure can be controlled depends on the pump speed. In Fig. 5, transient response of the LCV is shown for a ramp duty input. It is noted from Fig. 5 that the line pressure shows hysteresis for a rampwise ascending and descending duty input. It is seen from Fig. 4 - Fig. 5 that the simulation results are in good accordance with the experimental results, which demonstrates the validity of the LCV model.

In order to obtain the dynamic model of the

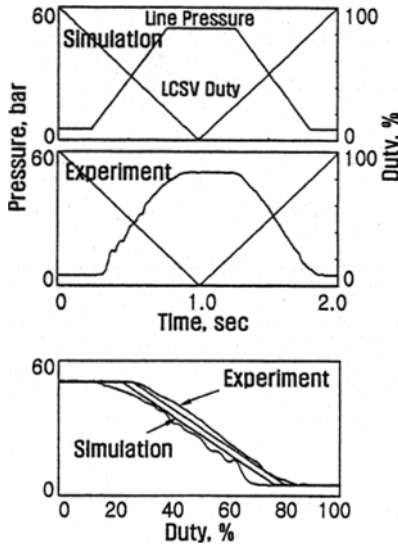


Fig. 5 Transient state characteristics of LCV

RCSV, it is necessary to consider the ineffective duty region of the VFS and the oil flow to and from the actuator during the shift. In Fig. 6, the RCV dynamic model is shown. As shown in Fig. 6, the RCSV is modeled as a second order system which produces the RCV spool displacement for a given duty input. The RCV inlet and exhaust port area are determined from the spool displacement x . Consequently, the RCV is modeled as an orifice area generator. The oil flow to and from the primary actuator, Q_{pin} and Q_{pout} can be calculated as follows,

$$Q_{pin} = C_d A_{in} \text{sign} \sqrt{|P_s - P_p|} \quad (4)$$

$$Q_{pout} = C_d A_{out} \text{sign} \sqrt{|P_p|} \quad (5)$$

State space equation of the primary pressure is represented as,

$$P_p = \frac{\beta}{V_p + A_p X_{pp}} \left(Q_{pin} - Q_{pout} - A_p \frac{dX_{pp}}{dt} \right) \quad (6)$$

where the last term in Eq. (6) represents the oil flow change occurred during the shift. dX_{pp}/dt is the movable flange speed. dX_{pp}/dt can be obtained from the shift speed and the CVT geometry as,

$$\frac{dX_{pp}}{dt} = \frac{di}{dt} \cdot \frac{dX_{pp}}{di} \quad (7)$$

In Fig. 7, performance characteristics of the RCV by the simulation are compared with the

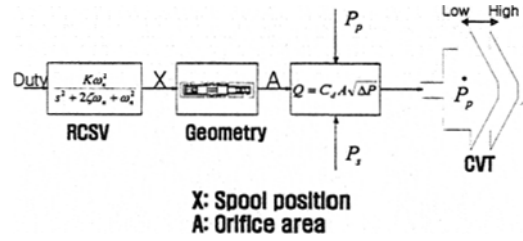


Fig. 6 Dynamic model of RCV

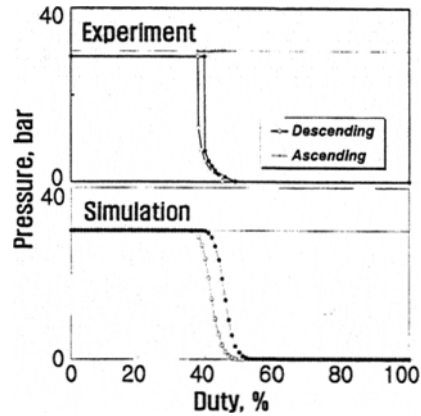


Fig. 7 Steady state characteristics of RCV

experiment. From Fig. 7, the effective duty range where the primary pressure can be controlled is observed as 38~50 % in the simulation and the experiment. It is considered that the effective duty range is so narrow that the RCV seems to operate like an on-off valve, which may cause a pressure pulsation in the primary actuator. As shown in Fig. 7, the simulation results agree with the experiment.

4. Line Pressure and Ratio Control Algorithm

In order to perform a CVT shift, the ratio control is needed together with the line pressure control, which requires low level controllers for the line pressure and the CVT ratio. Line pressure controller should be designed by considering the ineffective duty range of the LCSV since the line pressure shows an overshoot or undershoot when the duty signal changes from the ineffective range to the effective range. In this study, an anti-

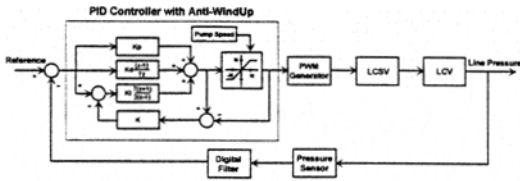


Fig. 8 Block diagram of line pressure control

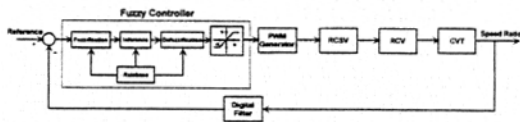


Fig. 9 Block diagram of CVT ratio fuzzy control

windup PID controller is suggested by considering the characteristics of the effective duty range of the LCV with changing anti-windup range with respect to the pump speed. The anti-windup duty range is selected as 20~80% from the experimental results in Fig. 4 and Fig. 5. Figure 8 shows a block diagram of the line pressure control.

As for the ratio control, a fuzzy logic based ratio controller is designed using the dynamic models of the RCV including the CVT shift dynamics. The fuzzy control logic was adopted by considering nonlinear characteristics of the CVT shift dynamics and the on-off characteristics of the RCV. The fuzzy controller calculates RCSV duty and compensate the error between the reference ratio and the actual ratio. In Fig. 9, a block diagram of the CVT ratio fuzzy control is shown. The fuzzy control gains were obtained based on the simulations and the final control gains were determined through the experiments. In the fuzzy logic, considering the RCV characteristics, it is designed that computation time which calculates the error of the ratio and the rate of the error can be changed depending on the velocity of the rate of the CVT ratio.

5. Investigation on Shift Performance

In Fig. 10, a schematic diagram of the experimental apparatus for the metal belt CVT is shown. The experimental apparatus consists of six modules; electric controlled CVT valve body and

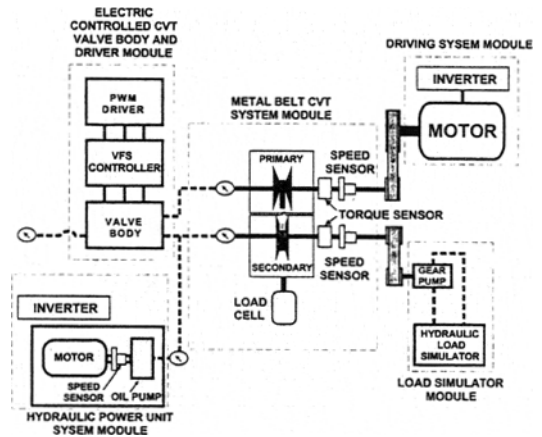


Fig. 10 Experimental apparatus

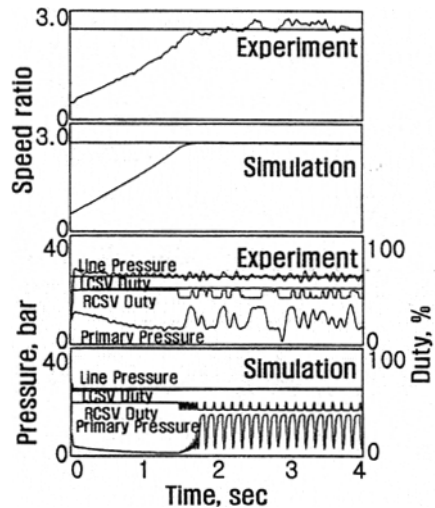


Fig. 11 Comparison of experimental results with simulation results

driver module, metal belt CVT system module, hydraulic power unit module, driving system module, load simulator module, and control system module. A variable speed A. C motor drives the primary pulley and power is transmitted to the secondary pulley via metal V-belt. The input torque is balanced with the load torque in the load simulator. Various speed ratios can be obtained by adjusting the primary thrust in the driving pulley.

Figure 11 shows comparison of the experimental results with the simulation when the speed ratio changes from $i=0.49$ to $i=2.48$. Both the experiments and the simulations are carried

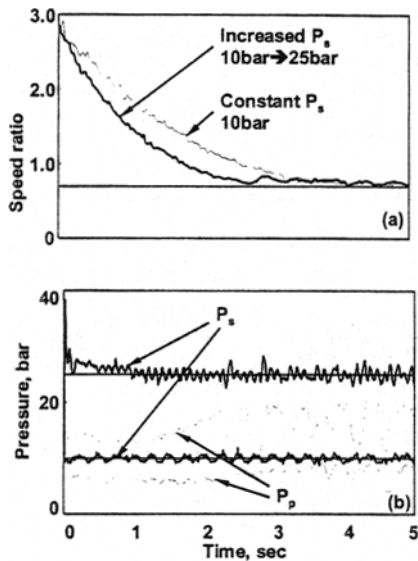


Fig. 12 Experimental results for upshift

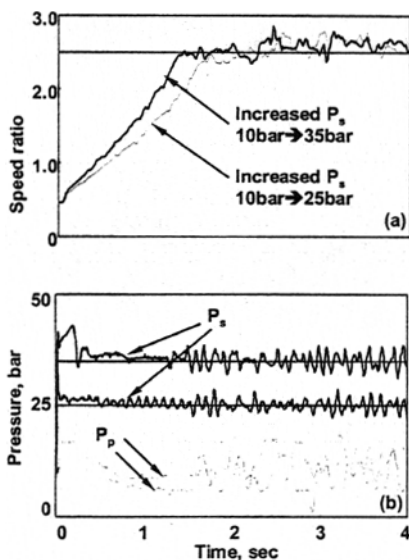


Fig. 13 Experimental results for downshift

out using the model based controllers designed for the line pressure and the ratio control. It is seen from Fig. 11 that response of the speed ratio and the primary pressure by the simulation agree well with the experimental results.

Figures 12 and 13 show the experimental results for the CVT shift performance. The experiments were performed based on the shift speed map and the low level controllers obtained

in this study. In Fig. 12, the CVT shift responses are shown for the upshift case. The fuzzy logic based ratio control was used to change the speed ratio from $i=2.48$ to $i=0.7$. The shift response when the line pressure is increased from $P_s=10$ bars to $P_s=25$ bars shows faster response than that of the constant line pressure, $P_s=10$ bars. It is seen from Fig. 12 that the primary pressure varies to follow the target speed ratio. In Fig. 13, shift response for the downshift is shown. Normally, in a CVT downshift, an increased belt clamping force, i. e. increased line pressure is required. It is noted from Fig. 13 that the shift response when P_s is increased from $P_s=10$ bars to $P_s=35$ bars shows faster response than that of the increased line pressure to 25 bars.

It is found from Fig. 12~13 that the CVT shift speed can be increased by increasing the line pressure. However, as mentioned earlier, an increased line pressure may cause an extra hydraulic loss, and the effect of increased line pressure on the fuel economy should be considered separately.

6. Conclusions

A CVT line pressure control strategy to improve the shift speed is suggested based on the shift speed maps constructed at each speed ratio for various line pressures. In addition, simplified dynamic models of the line pressure control valve (LCV) and the ratio control valve (RCV) for an electronically controlled metal belt CVT are presented. Based on the experimental results, the LCV and the ratio control solenoid valve are modeled as a second order system for a given duty input, and the RCV is modeled as an orifice area generator. The CVT shift dynamics is considered by introducing a flow change during the shift. Using the simplified dynamic models, an anti wind-up PID line pressure control algorithm and a fuzzy logic based ratio control algorithm are suggested. It is found that the simulation results by the model based control are in accordance with the experiments. Using the shift speed map and the simplified dynamic models of the hydraulic control valves obtained, shift

performances of the CVT are investigated. It is found from the experimental and the simulation results that improved shift speed can be achieved by increasing the line pressure.

Reference

- Fujii, T., Kurokawa, T. and Kanehara, S., 1993, "A Study of a Metal Pushing V-Belt Type CVT-Part 1: Relation Between Transmitted Torque and Pulley Trust," SAE 930666, pp. 1~11.
- Funatsu, K., Koyama, H. and Aoki, T., 1996, "Electronic Control System of Honda CVT," *Proc. Of Int. Conf. on Continuously Variable Power Transmissions 9636312*, pp. 43~49.
- Ide, T., Udagawa, A. and Kataoka, R., 1995, "Simulation Approach to the Effect of the Ratio Changing Speed of a Metal V-belt CVT on the Vehicle Response," *Int. J. of Vehicle System Dynamics*, Vol. 24, pp. 377~388.
- Kim, T. and Kim, H., 2000, "Low Level Control of Metal Belt CVT Considering Shift Dynamics and Ratio Valve On-Off Characteristics," *KSME International Journal*, Vol. 14, No. 6, pp. 645~654.
- Lee, H. and Kim, H., 2000, "Analysis of Primary and Secondary Thrusts for A Metal Belt CVT-Part I : New Formula for Speed Ratio-Torque-Thrust Relationship Considering Band Tension and Block Compression," *SAE 2000-01-0841*, pp. 1~9.
- Sato, K., Sakakiyama, R. and Nakamura, H., 1996, "Development of Electronically Controlled CVT System Equipped with CVTip," *Proc. of Int. Conf. on Continuously Variable Power Transmissions*, pp. 53~58.